



Published in final edited form as:

Mucosal Immunol. 2021 January ; 14(1): 209–218. doi:10.1038/s41385-020-0280-z.

NMP4 regulates the innate immune response to influenza A virus infection

Shuangshuang Yang^{1,2}, Michele Adaway³, Jianguang Du¹, Shengping Huang^{4,#}, Jie Sun⁴, Joseph P. Bidwell^{3,*}, Baohua Zhou^{1,2,*}

¹Department of Pediatrics, Herman B Wells Center for Pediatric Research, Indiana University School of Medicine, Indianapolis, Indiana, United States of America

²Department of Microbiology and Immunology, Indiana University School of Medicine, Indianapolis, Indiana, United States of America

³Department of Anatomy and Cell Biology & Physiology, Indiana University School of Medicine, Indianapolis, Indiana, United States of America

⁴Thoracic Diseases Research Unit, Division of Pulmonary and Critical Care, Department of Medicine, Mayo Clinic College of Medicine, Rochester, Minnesota, United States of America.

Abstract

Severe influenza A virus infection typically triggers excessive and detrimental lung inflammation with massive cell infiltration and hyper-production of cytokines and chemokines. We identified a novel function for nuclear matrix protein 4 (NMP4), a zinc-finger-containing transcription factor playing roles in bone formation and spermatogenesis, in regulating antiviral immune response and immunopathology. *Nmp4*-deficient mice are protected from H1N1 influenza infection, losing only 5% body weight compared to a 20% weight loss in wild type mice. While having no effects on viral clearance or CD8/CD4 T cell or humoral responses, deficiency of *Nmp4* in either lung structural cells or hematopoietic cells significantly reduces the recruitment of monocytes and neutrophils to the lungs. Consistent with fewer innate cells in the airways, influenza-infected *Nmp4*-deficient mice have significantly decreased expression of chemokine genes *Ccl2*, *Ccl7* and *Cxcl1* as well as pro-inflammatory cytokine genes *Il1b* and *Il6*. Furthermore, NMP4 binds to the promoters and/or conserved non-coding sequences of the chemokine genes and regulates their expression in mouse lung epithelial cells and macrophages. Our data suggest that NMP4 functions to promote monocyte- and neutrophil-attracting chemokine expression upon influenza A infection, resulting in exaggerated innate inflammation and lung tissue damage.

Users may view, print, copy, and download text and data-mine the content in such documents, for the purposes of academic research, subject always to the full Conditions of use:http://www.nature.com/authors/editorial_policies/license.html#terms

*Corresponding author: jbidwell@iu.edu (JPB), zhou@iu.edu (BZ).

#Current address: Department of Basic Medical Science, School of Medicine, University of Missouri Kansas City, Kansas City, MO 64108

Author Contribution

Conceptualization, S.Y., J.S., J.P.B. and B.Z.; Investigation, S.Y., M.A., J.D., S.H.; Data Analysis, S.Y., J.P.B. and B.Z.; Writing – original draft, S.Y.; Writing – review and editing, S.Y.; J.S., J.P.B. and B.Z.; Funding acquisition, J.P.B. and B.Z.; Supervision, J.P.B. and B.Z.

Disclosure

The authors declare no conflict of interests.

Introduction

Respiratory illnesses caused by influenza virus infection are one of the most common health threats in the world. Seasonal influenza results in about 3–5 million illnesses and 290,000 to 650,000 deaths every year. In the United States alone, at least 140,000 hospitalizations are estimated annually since 2010, representing a major impact on public health and economic burden.

Among the four types of viruses (A, B, C, D), influenza A viruses (IAV) account for most pandemics. The primary target of IAV is the airway and alveolar epithelial cells that cover the whole mucosal surface to provide the first line of defense against the inhaled pathogens¹. In addition to acting as a physical barrier, airway epithelial cells actively regulate both innate and adaptive immunity through the production of pro-inflammatory cytokines and chemokines that recruit and activate innate immune cells such as monocytes/macrophages and neutrophils to the lungs^{2–4}. The subsequently activated adaptive immunity contributes to virus clearance and long-term protection^{5–8}. While adequate influenza-induced inflammation is indispensable for the priming adaptive immune responses and control of virus proliferation, a growing number of studies suggest that exaggerated inflammation is associated with lung damage and death⁹. Indeed, patients with severe disease have extensive inflammatory infiltrates and increased cytokine production¹⁰. Mice deficient in some cytokines or their receptors show reduced morbidity and delayed mortality^{11, 12}. Therefore, maintaining a balance between eliminating the virus and controlling excessive inflammation is critical.

Nuclear matrix protein 4 (NMP4), also known as CAS-interacting zinc finger protein (CIZ) or Zinc finger protein 384 (ZNF384), was initially characterized as a parathyroid hormone (PTH)-responsive nuclear matrix architectural transcription factor that regulates gene activity by bending DNA^{13–15}. *Nmp4*-deficient mice challenged with anabolic stimuli such as PTH and BMP2 showed enhanced and accelerated bone formation^{13, 16–19}. In addition, *Nmp4*-deficiency resulted in sporadic infertility of male mice due to increased occurrence of spermatogenic apoptosis²⁰. Though expressed in a broad spectrum of tissues, its roles in the immune system are barely studied. Recently, *Nmp4* has been identified as a fusion partner with several genes to be associated with a subgroup of B-cell precursor acute lymphoblastic leukemia in childhood, with a frequency of approximately 3–4%^{21–24}. *Nmp4*-deficiency reduced the severity of serum-induced arthritis²⁵. NMP4 protein directly binds to pro-inflammatory cytokine IL-1 β promoter and activates its transcription, suggesting that *Nmp4* plays a role in regulating tissue inflammation²⁵.

In this study, we demonstrated that *Nmp4*-deficient mice were protected against H1N1 influenza A virus infection with significantly reduced body weight loss. The *Nmp4*-deficient mice had comparable viral clearance and adaptive immune responses to IAV infection but significantly fewer monocytes and neutrophil infiltration, and lower pro-inflammatory cytokine and chemokine production compared with wild type mice. NMP4 in both lung structural cells and hematopoietic cells contributes to monocytes and neutrophil recruitment after influenza infection. We further demonstrated that NMP4 bound to the promoter and/or conserved non-coding sequences of chemokines *Ccl2*, *Ccl7* and *Cxcl1* to regulate their

expression in mouse lung epithelial cells and bone marrow derived macrophages. Taken together, our data suggest that *Nmp4* participates in airway mucosal innate immune responses to influenza A viruses through regulation of chemokine expression in lung epithelial cells and macrophages.

Results

***Nmp4*^{-/-} mice showed reduced body weight loss after influenza infection.**

NMP4 is a zinc finger containing transcription factor and has been shown to bind to the promoter of the *Il1b* gene to regulate its expression²⁵. RNA-Seq analysis of the transcriptome in mesenchymal stem/progenitor cells²⁶ revealed that *Nmp4*-deficiency significantly altered expression of genes of several pathways involved in immune responses (Fig. S1A). Notably, the expressions of several chemokines were significantly changed (Fig. S1B). We, therefore, hypothesize that NMP4 plays a role in host defense against pathogens.

To characterize the role of NMP4 on anti-viral immune responses, we infected wild type (WT) and *Nmp4*-deficient mice with a sublethal dose of influenza virus strain A/Puerto Rico/8/1934 (PR8) and recorded their body weight loss. *Nmp4* knockout mice showed less morbidity and lost only 5% of original body weight compared to 20% of weight loss in WT mice (Fig. 1A). Surprisingly, quantitative RT-PCR (qRT-PCR) analysis of viral nucleoprotein (NP, Fig 1B) and polymerase (PA, Fig. S2A) RNA showed no difference in viral load in the lungs of *Nmp4*-deficient and WT mice at both 4 and 7 days post-infection (dpi), although *Nmp4*-deficient mice had slightly but significantly lower viral load at 10 dpi (Fig. 1B). Similar results were obtained by measuring the infectious virions in the bronchoalveolar lavage (BAL) fluid collected from mice (Fig. 1C and Fig. S2B). These data suggested that the reduced susceptibility of *Nmp4*-deficient to IAV infection was not due to a difference in viral clearance.

***Nmp4* is not required for adaptive immune responses to IAV infection**

The adaptive immune responses are critical to protecting the host from influenza virus infection as *Rag*-deficient mice failed to clear the virus resulting in sustained airway damage and death²⁷. To understand the mechanisms of enhanced protection in *Nmp4*-deficient mice, we first examined the adaptive immune responses to influenza infection. T cell responses normally peak at 6–9 days post-infection then resolve, whereas serum and mucosal antibody titers are sustained for a longer time²⁸. BAL fluid, lungs, lung-draining mediastinal lymph nodes (dLN) and spleens were collected from virus-infected mice at 7 and 10 dpi and stained with virus-specific tetramers to elucidate CD8 and CD4 T cell responses both locally and globally. Three of the five lung lobes were digested with collagen and DNase, disassociated with C tubes on a gentleMACS Dissociator (Miltenyi). The cells were stained with fluorescence-conjugated antibodies immediately and analyzed with flow cytometry (Fig. 2A). No significant differences were observed in the percentage of PA-tetramer positive CD8 T cells at 7 or 10 dpi (Fig. 2B). Similarly, total CD4 T cells in different tissues were also comparable between wild type and *Nmp4*-deficient mice (Fig. 2C).

Since CD8 and CD4 T cells contribute to viral control by producing effective cytokines, such as IFN- γ ^{6, 8}, we wondered whether *Nmp4* deficiency could possibly change the functionality of T cells in the infected lung. Mononuclear cells in lung single cell suspensions at day 10 post-viral infection were further isolated by Ficoll gradient centrifugation, and re-stimulated with phorbol 12-myristate 13 acetate (PMA) and ionomycin followed by the intracellular cytokine staining to examine IFN γ and TNF α production in lung infiltrating CD8 and CD4 T cells. Percentages of IFN- γ ⁺ (Fig. 2D) and TNF- α ⁺ (Fig. 2E) CD8 and CD4 T cells were similar in *Nmp4*-deficient and WT mice. We further examined cytokine production by virus-specific CD8 T cell in the lung using PA MHC class I tetramer provided by NIH Tetramer Core Facility at Emory University. No differences in IFN- γ and TNF- α production by PA⁺ CD8 T cells were observed (Fig. 2F). We further examined gamma interferon mRNA (*Ifng*) expression in the lungs of mice after IAV infection by quantitative RT-PCR. *Ifng* mRNA expression in both WT and *Nmp4*^{-/-} mice was upregulated at 7 dpi as adaptive immune responses reached a peak, yet no differences in expression levels were detected between these mice (Fig. 2G). ELISA quantification of IFN- γ in bronchoalveolar lavage fluid (BALF) also showed no difference.

Next, we assessed virus-specific antibodies in sera from virus-infected mice ELISA. WT and *Nmp4* deficient mice exhibited the similar amount of virus-specific IgG (Fig. 3A) and IgM (Fig. 3B) antibodies against the virus at both 7 and 10 dpi, indicating *Nmp4*-deficiency does not change B cell function and humoral immunity upon influenza virus infection. Taken together, our data suggest that NMP4 is not required for adaptive immune responses to influenza infection.

Reduced pro-inflammatory cytokine expression in lungs of *Nmp4* deficient mice.

During influenza infection, signals of infection recognized by pattern recognition receptors (PRRs) lead to the production of pro-inflammatory cytokines and chemokines^{4, 29}. An increasing number of studies suggested that pro-inflammatory cytokines and chemokines not only contribute to protective anti-viral immunity but also associate with tissue pathology and disease severity. Excessive cytokine production, termed cytokine storm, characterized by higher levels of pro-inflammatory cytokines and chemokines, is observed in patients hospitalized with severe influenza infections¹⁰. For example, IL-1 β was induced by influenza infection and blockade of IL-1 β receptor alleviated H1N1 induced inflammation³⁰. Similarly, IL-6 was associated with flu driven pathology¹⁰, even though studies also demonstrated the protective roles of IL-6 in promoting anti-viral immune responses^{31, 32}.

We first examined pro-inflammatory cytokine expression in the lungs of IAV infected *Nmp4*-deficient and WT mice. We found that *Il1b* but not *Il1a* mRNA expression in the lungs of *Nmp4*^{-/-} mice was significantly lower at 4 days post-infection comparing to that in the WT mice (Fig. 4A). Similarly, reduced *Il6* mRNA expression in the lung tissue and IL-6 in BALF of *Nmp4*^{-/-} mice were also observed at 4 dpi (Fig. 4B). Expression of other cytokines known to be involved in anti-viral immunity^{11, 33-35} including tumor necrosis factor (*Tnf*, Fig. 4C) and type I interferons (*Ifna1* and *Ifnb*, Fig. 4D) was not affected by *Nmp4* deficiency.

***Nmp4* is required for innate immune responses to influenza infection.**

Previous studies demonstrated that macrophages and neutrophils migrate rapidly to the airways upon influenza infection and contribute to both anti-viral immunity and immunopathology^{4, 29}. To determine the effects of *Nmp4* deficiency on innate immune responses, we examined the kinetics of monocytes/macrophages and neutrophils infiltrating into the lungs at increasing time points after infection. Total lung cellularity of *Nmp4*^{-/-} mice is significantly lower than that of WT mice at 4 and 7 dpi (Fig. 5A). Lung single cell suspensions were stained and analyzed by flow cytometry to phenotype the lung infiltrating myeloid cells (Supplementary Fig. S3). Both lung monocyte and neutrophil counts were significantly decreased in *Nmp4* deficient mice compared with WT mice at 4 dpi (Fig. 5B&C), with a trend of reduction of neutrophils at 7 dpi although this did not reach significance. Similarly, a trend towards fewer monocytes and significantly fewer neutrophils were also found in bronchoalveolar lavage fluid (BALF) of *Nmp4* deficient mice (data not shown).

To exclude the possibility that *Nmp4* deficiency impaired innate cell development, we analyzed monocytes and neutrophils in the bone marrow. The percentages and cell counts of monocytes and neutrophils in the bone marrow were similar between *Nmp4*^{-/-} and WT mice (Fig. 5E). Furthermore, percentages of monocytes and neutrophils in the blood were also comparable between these mice (Fig. 5F), suggesting the mobilization of these innate cells from bone marrow to blood was not affected by *Nmp4* deficiency.

Chemokines guide the migration of immune cells into the lung after infection. Consistent with reduced monocyte and neutrophil infiltration, we found that expression of several chemokines *Ccl2*, *Cxcl1* and *Ccl17* – known to attract monocytes and neutrophils – was attenuated in the lungs of *Nmp4*^{-/-} mice at 4 dpi (Fig. 5G–H) at mRNA level. CCL2 and CXCL1 protein concentrations in BALF at 4 dpi were also significantly different (Fig. 5G & H).

***Nmp4* in both lung structural cells and hematopoietic cells contributes to monocyte and neutrophil recruitment**

Since both lung epithelial cells and hematopoietic cells can secrete chemokines, we wondered which cell type is responsible for reduced innate immune responses after influenza infection. We generated bone marrow chimera mice by i.v. transfer of congenic marked bone marrow cells into lethally irradiated recipient mice. Bone marrow reconstitution was confirmed by flow cytometric analysis of peripheral blood mononuclear cells (PBMC) (supplementary Fig. S4). Four days after influenza infection, total viable lung cells in WT to KO group (where WT bone marrow cells were injected into irradiated *Nmp4* deficient recipients) were significantly reduced compared to the WT to WT group (Fig. 6A). Although not significant, KO to WT group also showed reduced total viable lung cell counts. Total viable lung cells were further reduced when both lung structural cells and hematopoietic cells deficient for *Nmp4* (KO to KO group) (Fig. 6A). Similar results were also seen when we gated on infiltrating monocytes (Fig. 6B) and neutrophils (Fig. 6C) that cell counts were significantly reduced when *Nmp4* was deficient in either lung structural cells or hematopoietic cells comparing to WT to WT group, and were further reduced when

Nmp4 was deficient in both lung structural cells and hematopoietic cells. Therefore *Nmp4* is required in both compartment to regulate anti-influenza innate immune responses in the lung.

***Nmp4* regulates chemokine expression in mouse lung epithelial cells and bone marrow derived macrophages**

Influenza virus primarily targets the respiratory epithelial cells including airway epithelial cells and pneumocytes. Influenza virus-infected epithelial cells release various chemokines to trigger the recruitment of an array of innate immune cells²⁹. Infiltrating monocytes/macrophages also express chemokines to recruit additional monocytes. We first examined NMP4 expression in the mouse lung by immunohistochemistry with a polyclonal rabbit antibody and demonstrated nuclear staining in airway epithelial cells, pneumocytes and macrophages in wild type mice but not *Nmp4* deficient mice (supplementary Fig. S5).

We next studied how *Nmp4* regulates innate cell attracting chemokine expression in lung epithelial cells and macrophages. We designed three guiding RNAs (gRNA1 – gRNA3) targeting the coding sequences of NMP4 N-terminus and cloned into the LentiCRISPR lentiviral vector³⁶ to edit the *Nmp4* gene in MLE-12 cells. MEL-12 cells transduced with the lentivirus expressing one of the gRNA, or mixture of the lentiviruses were cultured for 5 days in the presence of 20 µg/ml puromycin. Expression of NMP4 was examined by Western blot and cells transduced with one of three lentiviruses or their mixture showed reduced expression of NMP4 compared with control cells (Fig. 7A). Although puromycin selection yielded polyclonal lentivirus-transduced cells so that targeted gene would not be edited in 100% cells, gRNA1 showed the highest efficiency in knockdown of NMP4 expression. Therefore, gRNA1 lentivirus-transduced cells were chosen for the following studies. We used ChiP assay to test the binding of NMP4 to the promoters and conserved noncoding sequences (CNS) of *Ccl2*, *Cxcl1* and *Ccl7* genes that are down-regulated in influenza infected lungs of *Nmp4* deficient mice (Fig. 5G–I). The cells were also stimulated with poly I:C for 6 hours to test the effects of *Nmp4* knockdown/knockout on the mRNA expression of these chemokines using realtime PCR. In MLE-12 cells, we found that NMP4 bound to both *Ccl2* and *Cxcl1* gene loci (Fig. 7B, top and middle panels). Correlating to the NMP4 binding pattern, poly I:C stimulation up-regulated *Ccl2* and *Cxcl1* mRNA expression and *Nmp4* knockdown significantly reduced their expression (Fig. 7C). In bone marrow derived macrophages (BMDM), however, NMP4 did not bind to these two gene loci (Fig. 7D, top and middle panels). While poly I:C induced *Ccl2* mRNA expression independent of *Nmp4* (Fig. 7E, top panel), it did not induce *Cxcl1* expression in BMDM (Fig. 7E, middle panel). Different from *Ccl2* and *Cxcl1* induction and regulation, *Ccl7* expression in MLE-12 was not induced by poly I:C treatment and *Nmp4* knockdown showed minimal effect on its expression (Fig. 7C, bottom panel), while NMP4 had strong binding to the *Ccl7* promoter region in BMDM (Fig. 7D, bottom panel) and poly I:C treatment induced high *Ccl7* mRNA expression that was significantly reduce in *Nmp4* deficient BMDM (Fig. 7E, bottom panel).

To further confirm the regulation of *Ccl2* gene activity by NMP4, we cloned a 2.7 kb genomic fragment containing the CNS and promoter of the *Ccl2* gene into a pGL4Luc-RLuc dual luciferase reporter vector (Fig. 7F) and performed luciferase assay in MLE-12 cells

(Fig. 7G). While poly I:C treatment significantly induced *Ccl2* CNS+promoter driven luciferase activity, gRNA1 mediated *Nmp4* knockdown significantly reduced luciferase activity (Fig. 7G). Similar effects on *Ccl2* and *Cxcl1* mRNA expression and luciferase activity were also observed in siRNA mediated *Nmp4* knockdown MLE-12 cells (supplementary Fig. S6). We also performed *Ccl2* luciferase assay in BMDM. Consistent with the NMP4 independent expression of *Ccl2* in BMDM (Fig. 7E, top panel), *Ccl2* CNS +promoter driven luciferase activity was not reduced in *Nmp4*^{-/-} BMDM (data not shown). Taken together, our in vitro data indicate that NMP4 is able to bind to *Ccl2*, *Cxcl1* and *Ccl7* regulatory elements in mouse lung epithelial cells and/or BMDM to regulate chemokine expression in the lung.

Discussion

An overactive immune response causing severe tissue damage is an important contributor to death during exposure to highly virulent strains of influenza A such as the 1918 H1N1 virus or highly pathogenic avian H5N1 viruses. Mice infected with the highly pathogenic 1918 pandemic H1N1 virus exhibit significantly higher numbers of monocytes/macrophages and neutrophils in the lungs compared to mice infected with low pathogenic viruses². In this study, we demonstrated that mice deficient in the *Nmp4* gene that encodes a zinc finger transcription factor protected mice from H1N1 influenza virus-induced morbidity by recruiting significantly fewer monocytes/macrophages and neutrophils without significant impact on adaptive immune responses and viral clearance. Expression of monocyte and neutrophil attracting chemokines *Ccl2*, *Ccl7*, and *Cxcl1* was significantly reduced in the virus-infected airways of *Nmp4*-deficient mice. We further demonstrated that NMP4 in both lung structural cells and hematopoietic cells contributes to monocytes and neutrophil recruitment upon influenza infection. Mechanistically, NMP4 may directly bind to the *Ccl2*, *Cxcl1* and *Ccl7* gene loci to regulate the expression of these chemokines in lung epithelial cells and/or macrophages. Our data identify a novel function of NMP4 regulating chemokine expression in airway epithelial cells and macrophages to coordinate antiviral innate immune responses after influenza A virus infection.

Several papers reported that PR8 infection strongly induces the release of MCP1 (encoded by *Ccl2* gene) followed by monocyte recruitment and that CCL2 receptor-deficient mice displayed abrogated immunopathology^{12, 37-39}. In parallel, the CCL2 receptor CCR2-dependent recruitment of inflammatory macrophages contributes substantially to lung damage⁴⁰, and administration of a CCL2 blocking antibody can decrease mortality and morbidity following influenza A virus infection⁴¹. Upon influenza virus infection, airway epithelial cells induce CCL2 expression starting at 1 dpi and inflammatory monocytes/macrophages isolated at 3 dpi also produce CCL2⁴¹. *Nmp4* deficiency does not suppress *Ccl2* expression in bone marrow-derived macrophages (Fig. 7E) but the knockdown of *Nmp4* expression significantly reduces poly I:C-induced *Ccl2* expression in lung epithelial cells (Fig. 7C), strongly suggesting that regulation of influenza virus induced *Ccl2* expression by NMP4 is mainly in airway epithelial cells. Similar to our notion that reduced *Ccl2* expression in airway epithelial cells is protective to influenza A virus infection, a recent paper also demonstrated that airway epithelial cell-specific A20 knockout mice had decreased CCL2 production and were protected from Influenza A virus infection⁴².

Neutrophils are the first immune cells recruited to the site of injury or infection. While crucial players in controlling bacterial and fungal infections, less is known for neutrophil function in antiviral immune responses or viral pathogenesis. In a ferret model, the migration of neutrophils into the lung occurs within hours of influenza infection⁴³. Depletion of neutrophils prior to infection with influenza A virus leads to increased mortality in mice, suggesting a protective role for neutrophils⁴⁴. Massive infiltration of neutrophils into the lungs during influenza virus infection can result in acute lung inflammation that can be abrogated by Ab-mediated blockade of CXCL1 receptor CXCR2⁴⁵. Similar to the case of inflammatory monocytes/macrophages discussed above, we also found that *Nmp4* deficient mice had reduced *Cxcl1* expression / CXCL1 production (Fig. 5H) and neutrophil load (Fig. 5C) in the airways upon influenza A virus infection. Knockdown of *Nmp4* expression in mouse lung epithelial cells significantly inhibited poly I:C-induced *Cxcl1* expression (Fig. 7C, middle panel) that would result in reduced neutrophil influx immediately following IAV infection⁴³.

Our analysis with bone marrow chimera mice demonstrated that influenza induced recruitment of monocytes and neutrophils relied on *Nmp4* activity in both lung structural cells and hematopoietic cells, *Nmp4* deficiency in either compartment resulted in fewer monocytes and neutrophils recruited into the infected lung (Fig. 6). Lung epithelial cells are the primary target of influenza virus infection and source of pro-inflammatory cytokines and chemokines that recruit and activate monocytes²⁹. Cytokines and chemokines released from recruited and activated monocytes will further augment inflammation and cell infiltration²⁹. Consistent with these results, we found that expression of monocyte-attracting *Ccl2* and neutrophil-attracting *Cxcl1* in lung epithelial cells are *Nmp4* dependent (Fig 7C, top and middle panels). In addition, bone marrow derived macrophages (BMDM) are also significant source of *Ccl2* albeit independent of *Nmp4* (Fig 7E, top panel) and another monocyte-attracting chemokine *Ccl7* is highly induced by poly I:C in BMDM. Reduced *Ccl2* expression by *Nmp4* deficient epithelial cells leads to reduced monocytes and neutrophil recruitment, and fewer monocytes results in lower *Ccl2* and *Ccl7* expression further limiting the inflammatory infiltration. To complement to our in vitro studies presented in this manuscript, we are currently crossing our newly generated *Nmp4* flox mice to perform detailed analysis to define the role of NMP4 in regulating chemokine and cytokine expression in different cell types during influenza infection.

In conclusion, our studies demonstrate that *Nmp4* deficiency has no effects on adaptive immune responses but dampens the expression of monocyte- and neutrophil-attracting chemokine *Ccl2*, *Cxcl1* and *Ccl7* expression in lung epithelial cells and/or macrophages after influenza infection. The reduction in chemokine production in lung epithelial cells limits the initial infiltration of inflammatory monocytes/macrophages and neutrophils, which in turn will further reduce inflammation and inflammatory cytokine production, thus protect the mice from influenza-induced cytokine storm and tissue damage.

Materials and Methods

Mice and influenza virus infection

Nmp4^{-/-} mice under C57BL/6J background and their WT littermates were maintained in our colony at Indiana University Bioresearch Facility, Indiana University School of Dentistry. The mouse-adapted influenza virus strain A/PR/8/34 (H1N1) was prepared as described and provided by Dr. Sun's lab at Mayo Clinic⁴⁶. Mice were infected intranasally with 335 Pfu of PR8 in serum-free DMEM medium (Gibco) after anesthetized with Ketamine/Xylazine.

Preparation of lung cells

Mouse lungs were perfused with 5 ml PBS injected through right ventricle of heart until the lung turned white. Lung lobes were cut into small pieces and incubated in 5 mL HEPES buffer with 0.5mg/mL collagenase type 4 (Worthington) for 45 minutes at 37°C. After digestion, lung tissues were transferred to C-tubes and further dissociated using the gentleMACS Dissociator (Miltenyi Biotec). Tissue samples then were passed through 70 µm cell strainer and washed with HEPES buffer. The red blood cells in lungs were lysed in ACK lysing buffer and resuspended in FACS buffer for flow cytometric analysis.

For intracellular cytokine staining of, lung single cells as prepared above were re-suspended in 4 mL HEPES buffer and 2 mL Ficoll-Paque™ PLUS (GE Healthcare) were gently underlaid. After centrifuging at 1800–2000 rpm for 15 minutes, lung cells at the interface were harvested, washed with HEPES buffer and pelleted in IMDM (Gibco) complete medium containing 10% FBS and 2% penicillin-streptomycin. These cells included both lymphocytes and myeloid cells. They were re-stimulated with PMA and ionomycin for 5 hours and Golgi inhibitor monensin (Biolegend) was added for the last 3 hours, followed by flow cytometry analysis.

cDNA synthesis and real-time PCR

mRNA from culture cells and lung homogenates were isolated with TRIzol reagent (Invitrogen) or RNeasy Mini Kit (QIAGEN) following the manufacturer's instructions. cDNA was synthesized using High Capacity cDNA Reverse Transcriptase Kit (Applied Biosystems). Quantitative real-time PCR was performed with Fast SYBR Green Master Mix (Applied Biosystems) on the 7500 Fast Real-time PCR System (Applied Biosystems). Delta CT values were calculated for each transcript in which β2m mRNA expression was used for normalization.

Virus titer

Madin-Darby canine kidney cells (MDCK) cells were seed in 96-well plate and allowed the cells to grow 80% confluent. Cells were treated with dilutions of BAL fluid from virus-infected mice. To generate the standard curve, dilutions of influenza virus stock with known titer were used. After 6-hour incubation at 37°C in a humidified atmosphere with 5% CO₂, infection supernatant in each well was removed and cells were washed with sterile PBS twice. Expression of viral gene *NP* and *PA* was detected by RT-qPCR. Virus titer was

calculated based upon the standard curves of *NP* or *PA* expression vs viral titer diluted from virus stock solution (Fig. S2B).

ChIP analysis

Mouse lung epithelial (MLE-12) cells were seeded into the 10cm dish and grew to 80% confluent at a density of 8×10^6 . Cells were cross-linked for 10 min with 1% formaldehyde and lysed by sonication. Cross-linked cells were precleared with herring sperm DNA, bovine serum albumin, and protein A/G plus agarose beads (Santa Cruz Biotechnology). Cell extracts were incubated with 6 μ g antibody against NMP4 (Sigma HPA004051) or normal IgG rabbit antibody overnight at 4°C. The immunocomplexes were precipitated with protein A/G agarose at 4°C for 2 hours, washed and eluted. Cross-links were reversed at 65°C overnight. ChIPed DNA was extracted with phenol-chloroform, re-suspended in H₂O, and analyzed by quantitative PCR.

Flow cytometry analysis

Cells isolated from the BALF and single cell suspension of lungs were stained with fluorochrome-conjugated antibodies CD45, CD11b, Ly6G, F4/80, CD11c, CD4, CD8 (Biolegend), SiglecF (BD Biosciences) or MHC-I tetramers, MHC-II tetramer (NIH Tetramer Core at Emory University). Cells were incubated with fluorochrome-conjugated antibodies for 30 minutes at room temperature prior to washing and fixing with 1% formaldehyde. For intracellular cytokine staining, splenocytes were re-stimulated with PMA and ionomycin for 5 hours and Golgi inhibitor monensin (Biolegend) was added for the last 3 hours. After re-stimulation, cells were stained with surface marker including viability dye, washed, fixed and permeabilized and stained with intracellular antibody IFN- γ (Biolegend) for 1 hour. Stained cells were analyzed on an Attune Flow Cytometer (Thermo Fisher).

CRISPR/Cas9 mediated NMP4 knockdown in MLE-12 cells

To knockdown NMP4 expression in MLE-12 cells, we identified three gRNAs targeting the N-terminus of NMP4 as following: 5'- ATGAGTCCTGTAGATGGTAC-3', 5'- TCAATTCTAACCCGTA CTTC-3' and 5'- ACGTAAGGGTCATTCATCTC-3'. DNA oligomers corresponding to these gRNAs were synthesized by IDT and annealed DNA oligomers were inserted to the downstream of U6 promoter of LentiCRISPRv2 plasmid (Addgene, plasmid # 52961) as described³⁶. Lentivirus were generated by co-transfection the LentiCRISPRv2, PAX2, and PMDG.2 plasmids into HEK 293 T cells using lipofectamine 3000 reagent (Invitrogen). Lentivirus was harvested 36 to 48 hours after transfection and filtered through 0.45 μ m filter for immediate use or store at 4 °C for at most 24 hours.

Mouse lung epithelial cells (MLE-12) were culture in 6-well plate in HITES media until 90% confluency. Culture media were replaced with 1 to 2 mL fresh HITES media and 1mL DMEM medium containing lentivirus collected above. Cells were infected with lentivirus by centrifuged at 2000rpm for 45 mins with the presence of 8 μ g/mL polybrene (Sigma-Aldrich). After spin, cells were incubated in 37 °C, 5% CO₂ overnight. The next morning, target cells were changed back to fresh HITES media for expansion for at least 6 hours. To

select infected cells, 2 µg/mL puromycin was added to the media for 3–5 days when non-infected MLE-12 cells that treated with same concentration of puromycin were all dead.

Western blot confirmation of NMP4 knockdown

MLE-12 cells were washed with cold PBS and lysed in 200 µl RIPA buffer containing protein inhibitors. Cells were then scraped in to 1.5 mL microfuge tube and sonicate for 10 seconds. Lysates were spined at 10,000 rpm for 10 mins and the supernatants were transferred to clean tubes. Protein concentration was determined by Pierce™ Detergent Compatible Bradford assay kit (Thermo Fisher Scientific) following the manufacturer's instructions.

Sample buffer (4X) containing DTT was added into each sample (final 1X) and heated at 100 °C for 8–10 mins. 20–30 µg samples in 20–30 µL were loaded to the Mini-Protein TGX gels (Bio-Rad) and run at 200V for about 1~ 1.5 hours. After running, proteins were transfer to nitrocellulose membrane through the half-wet system at 200–400 mA for 30 mins. The membrane was blotted with rabbit anti-mouse NMP4 antibody (1:1000 dilution) or mouse anti-actin IgG (1: 500 dilution) overnight at 4°C and imaged with ChemiDoc MP Imaging System (BioRad).

Generation of bone marrow derived macrophages

For the generation of bone marrow-derived macrophages (BMDM), bone marrow cells were cultured in complete DMEM medium with 10% FBS, 2% penicillin-streptomycin, 2 mM L-glutamine, 0.1 mM 2-Mercaptoethanol and 40 ng/mL M-CSF for 7 days.

Luciferase reporter assay

A 2.7kb fragment containing the conserved non-coding sequence (CNS) and promoter of *Ccl2* gene were amplified from mouse genomic DNA using the following primers. 5'-GCTAGCCTCGAGTGATGTTCTATCAGTCCTCACCCATTAC-3', 5'-GAGGCCAGATCTCTCTGAGGCAGCCTTTTATTGTTAGCCAG-3'. The amplified fragment was digested with restriction enzymes XhoI and BglII and cloned into pGL4Luc-Rluc dual luciferase plasmid (Addgene, plasmid #64034).

MLE-12 cells, control cells or NMP4 knockdown cells, were culture in 24-well plate until 80% confluency and then transfected with pGL4Luc-Rluc vector or reporter plasmid using TransIT-2020 reagent (Mirus). After 24 hours of incubation in transfection complex, cells were stimulated with poly (I:C) (5µg/mL) for 6 hours and cell extracts were obtained through passive lysis buffer. Luciferase activities were measured using dual luciferase reporter assay system (Promega) according to the manufacturer's instructions. Firefly values were then normalized to Renilla values.

Statistical analysis

Statistical analysis was performed using Prism software (GraphPad Software) by either unpaired two-tail Student *t*-test or two-way ANOVA with Bonferroni multiple comparisons. P values of <0.05 were considered significant, with values of < 0.01 considered highly significant.

Supplementary Material

Refer to Web version on PubMed Central for supplementary material.

Acknowledgements

The authors thank Drs Mark Kaplan and Janice Blum for critical reading of this manuscript. This work was supported by National Institutes of Health Grants R01 AR073739 to J.P.B. and R01 AI085046 to B.Z.

References

- Vareille M, Kieninger E, Edwards MR, Regamey N. The airway epithelium: soldier in the fight against respiratory viruses. *Clinical microbiology reviews* 2011; 24(1): 210–229. [PubMed: 21233513]
- Perrone LA, Plowden JK, Garcia-Sastre A, Katz JM, Tumpey TM. H5N1 and 1918 pandemic influenza virus infection results in early and excessive infiltration of macrophages and neutrophils in the lungs of mice. *PLoS Pathog* 2008; 4(8): e1000115. [PubMed: 18670648]
- Hashimoto Y, Moki T, Takizawa T, Shiratsuchi A, Nakanishi Y. Evidence for phagocytosis of influenza virus-infected, apoptotic cells by neutrophils and macrophages in mice. *J Immunol* 2007; 178(4): 2448–2457. [PubMed: 17277152]
- Iwasaki A, Pillai PS. Innate immunity to influenza virus infection. *Nat Rev Immunol* 2014; 14(5): 315–328. [PubMed: 24762827]
- Skountzou I, Satyabhama L, Stavropoulou A, Ashraf Z, Esser ES, Vassilieva E et al. Influenza virus-specific neutralizing IgM antibodies persist for a lifetime. *Clinical and vaccine immunology : CVI* 2014; 21(11): 1481–1489. [PubMed: 25165027]
- La Gruta NL, Turner SJ. T cell mediated immunity to influenza: mechanisms of viral control. *Trends Immunol* 2014; 35(8): 396–402. [PubMed: 25043801]
- Kim TS, Sun J, Braciale TJ. T cell responses during influenza infection: getting and keeping control. *Trends Immunol* 2011; 32(5): 225–231. [PubMed: 21435950]
- Hamada H, Bassity E, Flies A, Strutt TM, Garcia-Hernandez Mde L, McKinstry KK et al. Multiple redundant effector mechanisms of CD8+ T cells protect against influenza infection. *J Immunol* 2013; 190(1): 296–306. [PubMed: 23197262]
- de Jong MD, Simmons CP, Thanh TT, Hien VM, Smith GJ, Chau TN et al. Fatal outcome of human influenza A (H5N1) is associated with high viral load and hypercytokinemia. *Nat Med* 2006; 12(10): 1203–1207. [PubMed: 16964257]
- Oshansky CM, Gartland AJ, Wong SS, Jeevan T, Wang D, Roddam PL et al. Mucosal immune responses predict clinical outcomes during influenza infection independently of age and viral load. *Am J Respir Crit Care Med* 2014; 189(4): 449–462. [PubMed: 24308446]
- Perrone LA, Szretter KJ, Katz JM, Mizgerd JP, Tumpey TM. Mice lacking both TNF and IL-1 receptors exhibit reduced lung inflammation and delay in onset of death following infection with a highly virulent H5N1 virus. *J Infect Dis* 2010; 202(8): 1161–1170. [PubMed: 20815704]
- Dawson TC, Beck MA, Kuziel WA, Henderson F, Maeda N. Contrasting effects of CCR5 and CCR2 deficiency in the pulmonary inflammatory response to influenza A virus. *Am J Pathol* 2000; 156(6): 1951–1959. [PubMed: 10854218]
- Childress P, Stayrook KR, Alvarez MB, Wang Z, Shao Y, Hernandez-Buquer S et al. Genome-Wide Mapping and Interrogation of the Nmp4 Antianabolic Bone Axis. *Molecular endocrinology (Baltimore, Md)* 2015; 29(9): 1269–1285.
- Torrunguang K, Alvarez M, Shah R, Onyia JE, Rhodes SJ, Bidwell JP. DNA binding and gene activation properties of the Nmp4 nuclear matrix transcription factors. *J Biol Chem* 2002; 277(18): 16153–16159. [PubMed: 11867614]
- Rump K, Siffert W, Peters J, Adamzik M. The Transcription Factor NMP4 Binds to the AQP5 Promoter and Is a Novel Transcriptional Regulator of the AQP5 Gene. *DNA and cell biology* 2016; 35(7): 322–327. [PubMed: 27058007]

16. Childress P, Philip BK, Robling AG, Bruzzaniti A, Kacena MA, Bivi N et al. Nmp4/CIZ suppresses the response of bone to anabolic parathyroid hormone by regulating both osteoblasts and osteoclasts. *Calcified tissue international* 2011; 89(1): 74–89. [PubMed: 21607813]
17. He Y, Childress P, Hood M Jr., Alvarez M, Kacena MA, Hanlon M et al. Nmp4/CIZ suppresses the parathyroid hormone anabolic window by restricting mesenchymal stem cell and osteoprogenitor frequency. *Stem cells and development* 2013; 22(3): 492–500. [PubMed: 22873745]
18. Morinobu M, Nakamoto T, Hino K, Tsuji K, Shen ZJ, Nakashima K et al. The nucleocytoplasmic shuttling protein CIZ reduces adult bone mass by inhibiting bone morphogenetic protein-induced bone formation. *J Exp Med* 2005; 201(6): 961–970. [PubMed: 15781586]
19. Robling AG, Childress P, Yu J, Cotte J, Heller A, Philip BK et al. Nmp4/CIZ suppresses parathyroid hormone-induced increases in trabecular bone. *Journal of cellular physiology* 2009; 219(3): 734–743. [PubMed: 19189321]
20. Nakamoto T, Shiratsuchi A, Oda H, Inoue K, Matsumura T, Ichikawa M et al. Impaired spermatogenesis and male fertility defects in CIZ/Nmp4-disrupted mice. *Genes Cells* 2004; 9(6): 575–589. [PubMed: 15189450]
21. Hirabayashi S, Ohki K, Nakabayashi K, Ichikawa H, Momozawa Y, Okamura K et al. ZNF384-related fusion genes define a subgroup of childhood B-cell precursor acute lymphoblastic leukemia with a characteristic immunotype. *Haematologica* 2017; 102(1): 118–129. [PubMed: 27634205]
22. Qian M, Zhang H, Kham SK, Liu S, Jiang C, Zhao X et al. Whole-transcriptome sequencing identifies a distinct subtype of acute lymphoblastic leukemia with predominant genomic abnormalities of EP300 and CREBBP. *Genome research* 2017; 27(2): 185–195. [PubMed: 27903646]
23. Shago M, Ablu O, Hitzler J, Weitzman S, Abdelhaleem M. Frequency and outcome of pediatric acute lymphoblastic leukemia with ZNF384 gene rearrangements including a novel translocation resulting in an ARID1B/ZNF384 gene fusion. *Pediatric blood & cancer* 2016; 63(11): 1915–1921. [PubMed: 27392123]
24. Yaguchi A, Ishibashi T, Terada K, Ueno-Yokohata H, Saito Y, Fujimura J et al. EP300-ZNF384 fusion gene product up-regulates GATA3 gene expression and induces hematopoietic stem cell gene expression signature in B-cell precursor acute lymphoblastic leukemia cells. *International journal of hematology* 2017; 106(2): 269–281. [PubMed: 28378055]
25. Nakamoto T, Izu Y, Kawasaki M, Notomi T, Hayata T, Noda M et al. Mice Deficient in CIZ/NMP4 Develop an Attenuated Form of K/BxN-Serum Induced Arthritis. *Journal of cellular biochemistry* 2016; 117(4): 970–977. [PubMed: 26378628]
26. Shao Y, Wichern E, Childress PJ, Adaway M, Misra J, Klunk A et al. Loss of Nmp4 optimizes osteogenic metabolism and secretion to enhance bone quality. *American journal of physiology Endocrinology and metabolism* 2019.
27. Wu H, Haist V, Baumgartner W, Schughart K. Sustained viral load and late death in Rag2^{-/-} mice after influenza A virus infection. *Virology journal* 2010; 7: 172. [PubMed: 20667098]
28. Subbarao K, Murphy BR, Fauci AS. Development of effective vaccines against pandemic influenza. *Immunity* 2006; 24(1): 5–9. [PubMed: 16413916]
29. Pulendran B, Maddur MS. Innate immune sensing and response to influenza. *Current topics in microbiology and immunology* 2015; 386: 23–71. [PubMed: 25078919]
30. Kim KS, Jung H, Shin IK, Choi BR, Kim DH. Induction of interleukin-1 beta (IL-1beta) is a critical component of lung inflammation during influenza A (H1N1) virus infection. *J Med Virol* 2015; 87(7): 1104–1112. [PubMed: 25802122]
31. Lauder SN, Jones E, Smart K, Bloom A, Williams AS, Hindley JP et al. Interleukin-6 limits influenza-induced inflammation and protects against fatal lung pathology. *Eur J Immunol* 2013; 43(10): 2613–2625. [PubMed: 23857287]
32. Yang ML, Wang CT, Yang SJ, Leu CH, Chen SH, Wu CL et al. IL-6 ameliorates acute lung injury in influenza virus infection. *Sci Rep* 2017; 7: 43829. [PubMed: 28262742]
33. Jiang L, Yao S, Huang S, Wright J, Braciale TJ, Sun J. Type I IFN signaling facilitates the development of IL-10-producing effector CD8(+) T cells during murine influenza virus infection. *Eur J Immunol* 2016; 46(12): 2778–2788. [PubMed: 27701741]

34. Davidson S, Crotta S, McCabe TM, Wack A. Pathogenic potential of interferon alpha in acute influenza infection. *Nat Commun* 2014; 5: 3864. [PubMed: 24844667]
35. Sun J, Madan R, Karp CL, Braciale TJ. Effector T cells control lung inflammation during acute influenza virus infection by producing IL-10. *Nat Med* 2009; 15(3): 277–284. [PubMed: 19234462]
36. Shalem O, Sanjana NE, Hartenian E, Shi X, Scott DA, Mikkelsen T et al. Genome-scale CRISPR-Cas9 knockout screening in human cells. *Science* 2014; 343(6166): 84–87. [PubMed: 24336571]
37. Lin KL, Suzuki Y, Nakano H, Ramsburg E, Gunn MD. CCR2+ monocyte-derived dendritic cells and exudate macrophages produce influenza-induced pulmonary immune pathology and mortality. *J Immunol* 2008; 180(4): 2562–2572. [PubMed: 18250467]
38. Herold S, von Wulffen W, Steinmueller M, Pleschka S, Kuziel WA, Mack M et al. Alveolar epithelial cells direct monocyte transepithelial migration upon influenza virus infection: impact of chemokines and adhesion molecules. *J Immunol* 2006; 177(3): 1817–1824. [PubMed: 16849492]
39. Lin SJ, Lo M, Kuo RL, Shih SR, Ojcius DM, Lu J et al. The pathological effects of CCR2+ inflammatory monocytes are amplified by an IFNAR1-triggered chemokine feedback loop in highly pathogenic influenza infection. *J Biomed Sci* 2014; 21: 99. [PubMed: 25407417]
40. Herold S, Steinmueller M, von Wulffen W, Cakarova L, Pinto R, Pleschka S et al. Lung epithelial apoptosis in influenza virus pneumonia: the role of macrophage-expressed TNF-related apoptosis-inducing ligand. *J Exp Med* 2008; 205(13): 3065–3077. [PubMed: 19064696]
41. Kok WL, Denney L, Benam K, Cole S, Clelland C, McMichael AJ et al. Pivotal Advance: Invariant NKT cells reduce accumulation of inflammatory monocytes in the lungs and decrease immunopathology during severe influenza A virus infection. *J Leukoc Biol* 2012; 91(3): 357–368. [PubMed: 22003207]
42. Maelfait J, Roose K, Vereecke L, Mc Guire C, Sze M, Schuijs MJ et al. A20 Deficiency in Lung Epithelial Cells Protects against Influenza A Virus Infection. *PLoS pathogens* 2016; 12(1): e1005410. [PubMed: 26815999]
43. van den Brand JM, Stittelaar KJ, van Amerongen G, Reperant L, de Waal L, Osterhaus AD et al. Comparison of temporal and spatial dynamics of seasonal H3N2, pandemic H1N1 and highly pathogenic avian influenza H5N1 virus infections in ferrets. *PLoS One* 2012; 7(8): e42343. [PubMed: 22905124]
44. Tumpey TM, Garcia-Sastre A, Taubenberger JK, Palese P, Swayne DE, Pantin-Jackwood MJ et al. Pathogenicity of influenza viruses with genes from the 1918 pandemic virus: functional roles of alveolar macrophages and neutrophils in limiting virus replication and mortality in mice. *Journal of virology* 2005; 79(23): 14933–14944. [PubMed: 16282492]
45. Seki M, Kohno S, Newstead MW, Zeng X, Bhan U, Lukacs NW et al. Critical role of IL-1 receptor-associated kinase-M in regulating chemokine-dependent deleterious inflammation in murine influenza pneumonia. *J Immunol* 2010; 184(3): 1410–1418. [PubMed: 20042589]
46. Lawrence CW, Braciale TJ. Activation, differentiation, and migration of naive virus-specific CD8+ T cells during pulmonary influenza virus infection. *J Immunol* 2004; 173(2): 1209–1218. [PubMed: 15240712]

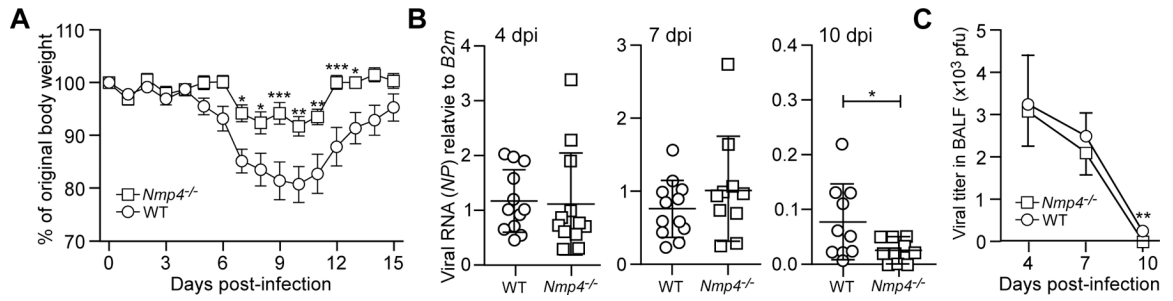


Figure 1. *Nmp4* deficiency reduces disease severity after H1N1 (PR8) influenza virus infection in mice.

(A) Body weight changes of mice after infection (n = 10 – 12 mice). **(B)** Realtime PCR quantification of influenza virus NP gene expression (relative to reference gene *B2m*) in the lung tissues at specified time points. **(C)** Viral titer in bronchoalveolar lavage fluid (n = 10 – 12 mice). Data represent mean ± SEM from one of four independent experiments. *: p < 0.05; **: p < 0.01; ***: p < 0.001 by two-way ANOVA with Bonferroni post-test (A&C) or two-tailed t-test (B).

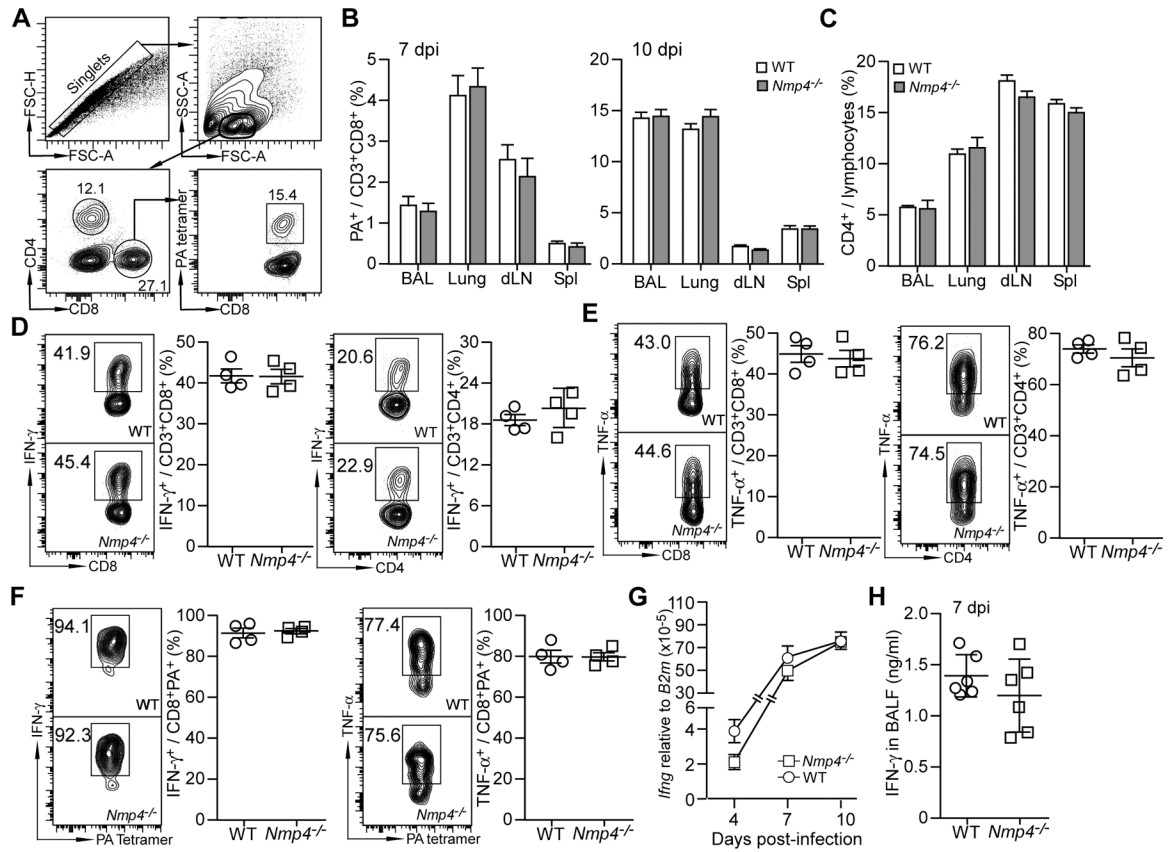


Figure 2. *Nmp4* deficiency does not affect adaptive immune response to influenza infection in mice.

(A) Gating strategy to identify CD4, CD8, and virus-specific (PA Class I tetramer) CD8 T cells in influenza infected lung. (B) Flow cytometric analysis of PA⁺ CD8 T cells in specified tissues at 7 and 10 dpi. (C) Flow cytometric analysis of total CD4 T cells in specified tissues at 7 dpi. (D) Flow cytometric analysis of IFN- γ expression by CD8 and CD4 T cells in the lung. (E) Flow cytometric analysis of TNF- α expression by CD8 and CD4 T cells in the lung. (F) Flow cytometric analysis of IFN- γ and TNF- α expression by virus-specific PA⁺ CD8 T cells in the lung. (G) Gamma interferon mRNA (*Ifng*) expression in the lung tissue was detected by qRT-PCR (n = 10 – 12 mice). *Ifng* mRNA expression was normalized to *B2m* expression. (H) Interferon gamma concentration in bronchoalveolar lavage fluid (BALF) obtained at 7 dpi. Data represent mean \pm SEM from one of two independent experiments. n = 10 mice for B and C. For D - F, plots were gated on live cells negative for Zombie dyes to minimize the interference of cells died during PAM and ionomycin re-stimulation. BAL: Bronchoalveolar lavage; dLN: Lung draining lymph nodes; Spl: Spleen.

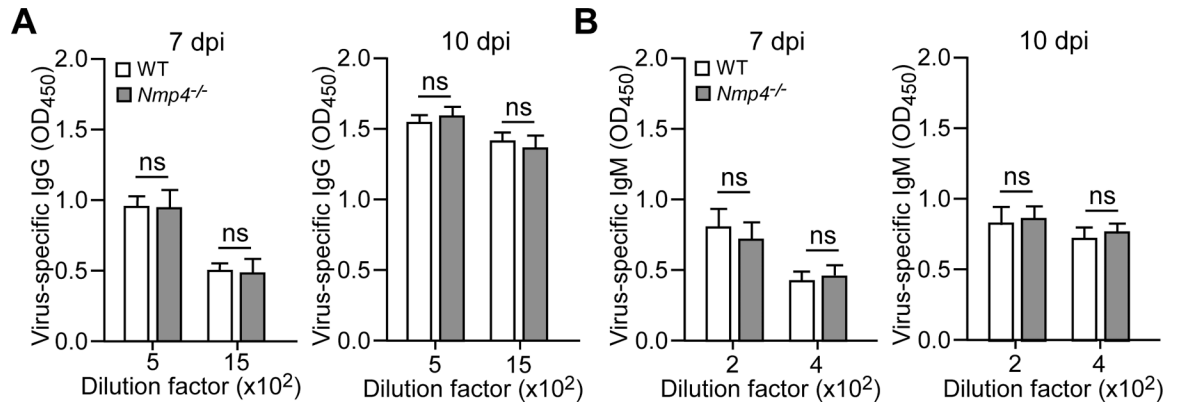


Figure 3. *Nmp4* deficiency does not affect humoral immune response to influenza infection in mice.

(A) ELISA quantification of serum influenza virus-specific IgG at 7 and 10 dpi. (B) ELISA quantification of serum influenza virus-specific IgM at 7 and 10 dpi. Data represent mean ± SEM (n = 10 – 12 mice) from one of two independent experiments. ns: not significant by one way ANOVA with Bonferroni post-test.

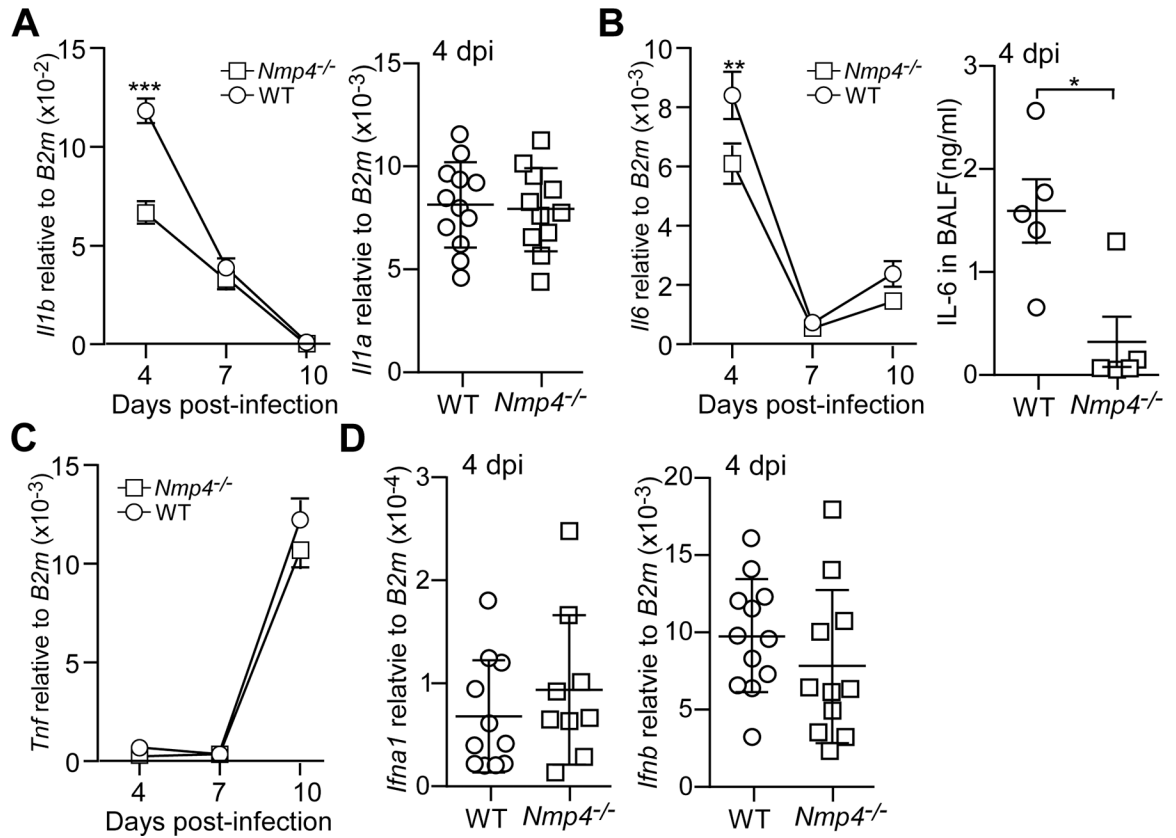


Figure 4. Effects of *Nmp4* deficiency on expression of cytokines in the lung tissues after influenza virus infection.

(A) qRT-PCR detection of *Il1b* and *Il1a* in lung tissues. (B) qRT-PCR detection of *Il6* in lung tissues and ELISA measurement of IL-6 in BALF. (C) qRT-PCR detection of *Tnf* in lung tissues. (D) qRT-PCR detection of *Ifna1* and *Ifnb* in lung tissues. Data represent mean \pm SEM (n = 10 – 12 mice) from one of two independent experiments. *: p < 0.05; ***: p < 0.001 by two-way ANOVA with Bonferroni post-hoc test.

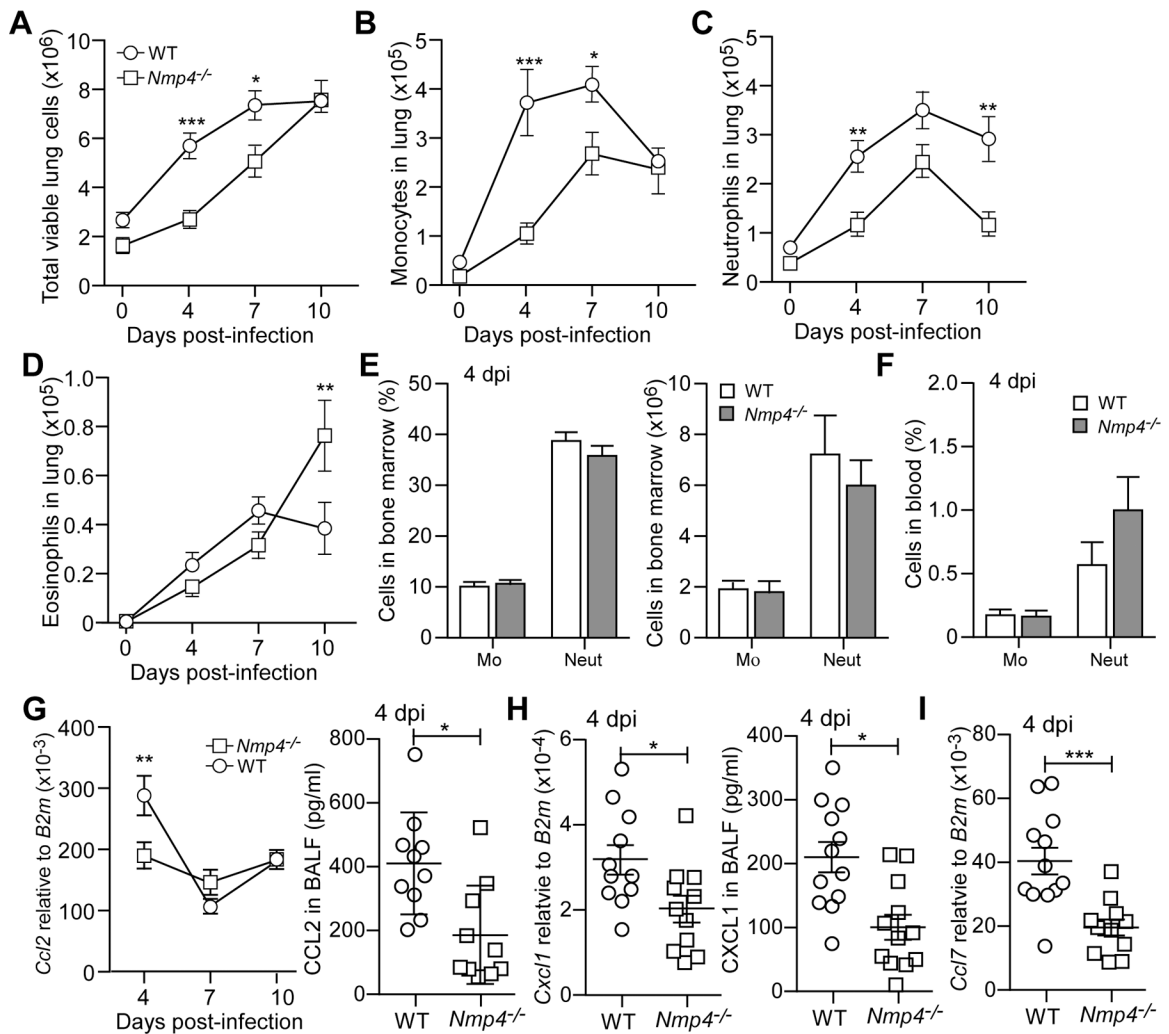


Figure 5. *Nmp4* deficient mice showed reduced innate immune response to influenza virus infection.

(A) Total viable cells in lung tissues after collagenase digestion. (B) Flow cytometric analysis of inflammatory monocytes/macrophages in lung tissues. (C) Flow cytometric analysis of neutrophils in lung tissues. (D) Flow cytometric analysis of eosinophils in lung tissues. (E) Flow cytometric analysis of monocytes and neutrophils in bone marrow. (F) Flow cytometric analysis of monocytes and neutrophils in blood. (G) Realtime PCR detection of *Ccl2* expression in the lung tissue and ELISA measurement of CCL2 concentration in BALF. (H) Realtime PCR detection of *Cxcl1* expression in the lung tissue and ELISA measurement of CXCL1 concentration in BALF. (I) Realtime PCR detection of *Ccl7* expression in the lung tissue. Data represent mean \pm SEM from one of four (A-D) or two (E-I) independent experiments. $n = 10 - 12$ mice for A-D & G, and $n = 4$ mice for E-F. *: $p < 0.05$; **: $p < 0.01$; ***: $p < 0.001$ by two-way ANOVA with Bonferroni post-test (A-G) or two tailed t-test (H & I).

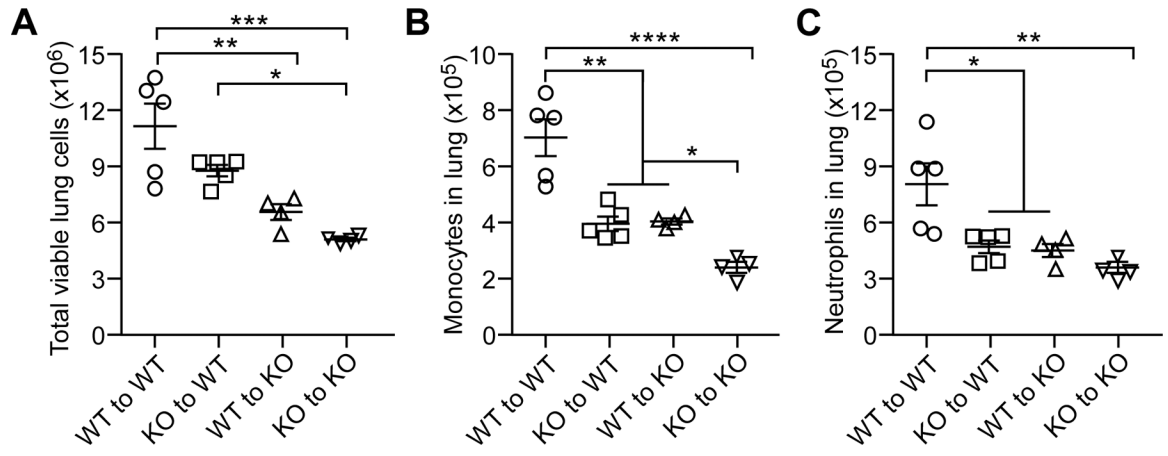


Figure 6. NMP4 in both bone marrow derived cells and lung structural cells regulates Innate immune response to influenza infection.

(A) Total viable cells in lung tissues 4 days after influenza infection. (B) Flow cytometric analysis of inflammatory monocytes/macrophages in lung tissues. (C) Flow cytometric analysis of neutrophils in lung tissues. Data represent mean ± SEM from one of two independent experiments. n = 4 – 5 mice. *: p < 0.05; **: p < 0.01; ***: p < 0.001; ****: p < 0.0001 by one-way ANOVA with Bonferroni post-test.

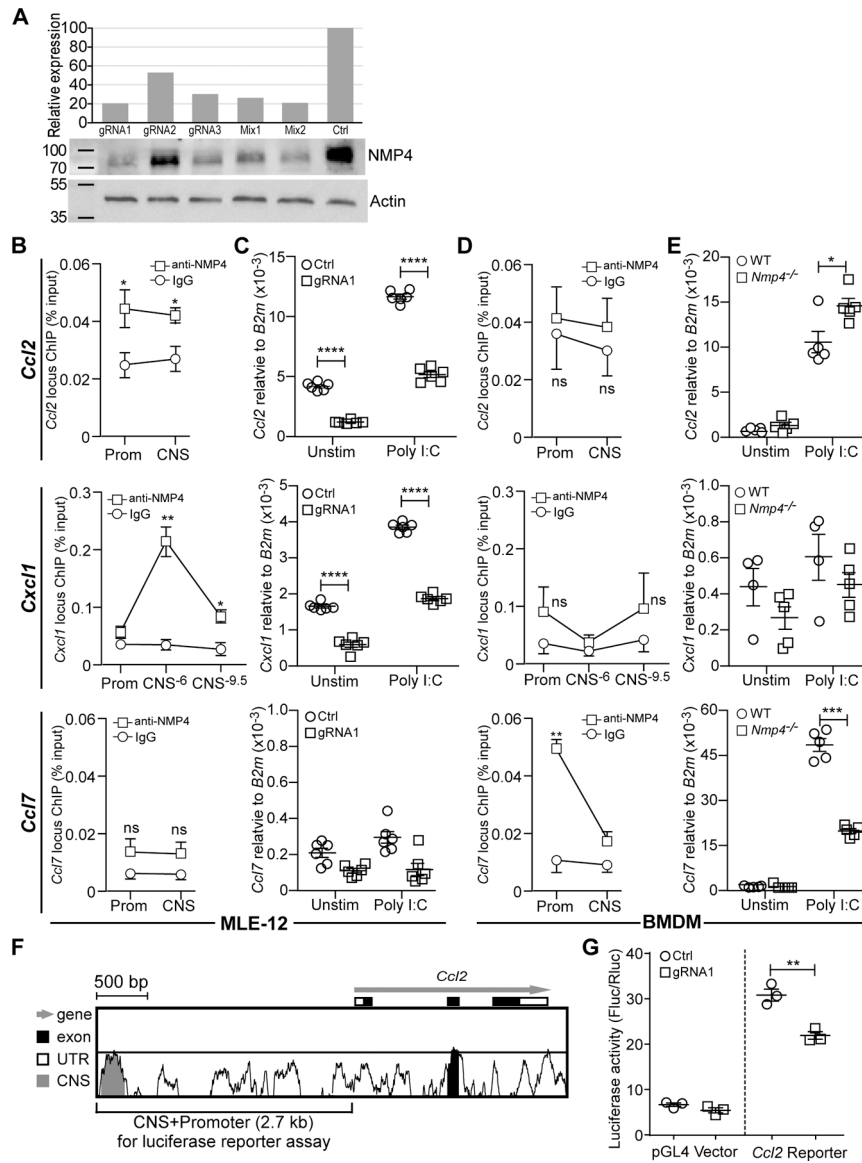


Figure 7. NMP4 regulates chemokine expression in mouse airway epithelial cells and bone marrow derived macrophages (BMDM)
 (A) Western blot to verify *Nmp4* knockdown in mouse lung epithelial cell line (MLE-12) transduced with lentiCRISPR lentivirus containing *Nmp4* targeting gRNA and selected with puromycin. (B) ChIP analysis of NMP4 binding to *Ccl2*, *Cxcl1* and *Ccl7* loci in MLE-12 cells. (C) Realtime PCR assessment of effects of *Nmp4* knockdown on *Ccl2*, *Cxcl1* and *Ccl7* expression in MLE-12 cells stimulated with poly I:C for 6 hours. (D) ChIP analysis of NMP4 binding to *Ccl2*, *Cxcl1* and *Ccl7* loci in BMDM. (E) Realtime PCR assessment of effects of *Nmp4* deficiency on *Ccl2*, *Cxcl1* and *Ccl7* expression in BMDM stimulated with poly I:C for 6 hours. (F) Alignment of mouse and human CCL2 gene locus showing gene structure and conserved non-coding sequence. The 2.7 kb fragment was cloned to the pGL4Luc-RLuc dual luciferase reporter vector. (G) Luciferase reporter assay to assess the effect of NMP4 knockdown on *Ccl2* promoter activity in MLE-12 cells. Data represent mean \pm SEM. n = 4 for ChIP (B&D) and luciferase assay (G); n = 6 for realtime PCR analysis of

chemokine expression (C&E). *: $p < 0.05$; **: $p < 0.05$ by one-way ANOVA with Bonferroni post-test. Prom: promoter region; CNS: conserved non-coding sequence; CNS⁻⁶ and CNS^{-9.5}: conserved non-coding sequences 6 kb and 9.5 kb upstream of *Cxcl1* transcription start site; UTR: untranslated region.